Article

Study on the Catalytic Characteristics of Precious Metal Catalysts with Different Pt/Pd Ratios for Soot Combustion

Diming Lou, Beihong Xiang, Yunhua Zhang,* Liang Fang, Piqiang Tan, and Zhiyuan Hu

Read Online

ACCESS | Metrics & More | Article Recommendations

ABSTRACT: Soot particles in engine exhaust seriously pollute the atmosphere and endanger human health. For soot oxidation, Pt and Pd precious metal catalysts are widely used and are effective. In this paper, the catalytic characteristics of catalysts with different Pt/Pd mass ratios for soot combustion were studied through X-ray diffraction, X-ray photoelectron spectroscopy (XPS), Brunauer–Emmett–Teller analysis, scanning electron microscopy, transmission electron microscopy, the temperature-programmed oxidation reaction, and thermogravimetry. Besides, the adsorption characteristics of soot and O_2 on the catalyst surface were explored by density functional theory (DFT) calculations. The research results showed that the activity of catalysts for soot oxidation from strong to weak is Pt/Pd = 10:1, Pt/Pd = 5:1, Pt/Pd = 1:0, and Pt/Pd = 1:1. XPS results showed that the concentration of oxygen vacancies in the catalyst is the highest when the Pt/Pd ratio is 10:1. The specific surface area of the catalyst increases first and then decreases with the increase of Pd content. When the Pt/Pd ratio is 10:1, the specific surface area and pore volume of the catalyst reach the maximum. The following are the DFT calculation results. With the increase of Pd content, the adsorption energy of particles on the catalyst surface decreases first and then increases. When the Pt/Pd ratio is 10:1, the adsorption of C on the catalyst surface is the strongest, and the adsorption of O_2 is also strong. In addition, this surface has a strong ability to donate electrons. The theoretical simulation results are consistent with the activity test results. The research results have a guiding significance for optimizing the Pt/Pd ratio and improving the soot oxidation performance of the catalyst.
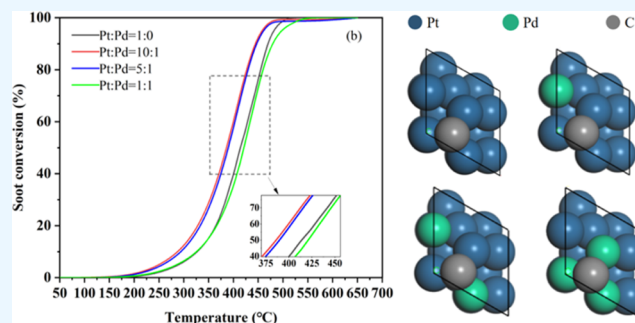
1. INTRODUCTION

The diesel engine with its high power, economy, and reliability is widely used in the field of heavy vehicles. After the combustible mixture in the diesel engine is compression-ignited, the combustion method is diffusion combustion. This method causes the soot and particulate matter emission from the diesel engine to be prominent, which seriously endangers the atmospheric environment and human health. Reducing diesel engine pollutant emissions is of great significance to its long-term development and environmental protection. According to the latest China Mobile Source Environmental Management Annual Report (2021) released by the Ministry of Ecology and Environment, diesel vehicles in China emitted 64,000 tons of particulate matter (PM) in 2020, accounting for more than 99% of total vehicle emissions. The problem of particulate air pollution is closely related to national economic construction and social development. In order to control the emission of particulate matter from mobile sources, strict emission laws and regulations have been formulated at home and abroad. At present, the emission regulations implemented in China are the National VI emission standards, which have strict requirements on the emission limits of PM. At the same time, the pre-researched Euro VII emission regulations will

further tighten the emission limit of particulate matter. The Euro VII emission proposal, issued by the European Commission on November 10, 2022, will tighten particulate matter limits for trucks and buses. Gradually strict emission regulations have prompted the development and innovation of diesel engine particulate matter emission control technology. The particulate matter emission control technologies mainly include in-machine purification and exhaust after-treatment. At present, the diesel particulate filter (DPF) is the most effective control technology for diesel particulate matter emissions.[1] DPF can only physically trap particulate matter. To completely remove particulate matter, DPF regeneration is required. Regeneration is divided into active regeneration and passive regeneration.[2] The research focus of passive regeneration is DPF-coated catalytic regeneration technology (catalytic diesel

particulate filter, CDPF).[3] The CDPF technology reduces the activation energy of particulate matter oxidation by coating the soot catalyst in DPF so that particulate matter can be oxidized at normal exhaust temperature. Therefore, the development of high-performance soot catalysts is the key to CDPF technology.

Soot catalysts mainly include precious metal catalysts, alkali metal catalysts, and transition-metal oxide catalysts.[4] The active components of precious metals mainly include Pt,[5−8] Pd,[9] Rh,[10] etc. And they are loaded on metal oxide supports such as aluminum to form commonly used supported-type precious metal catalysts. Precious metal catalysts have the advantages of high activity and long life. At present, the most widely used commercial CDPF catalysts are Pt catalysts. Researchers have done extensive research on their soot oxidation properties. The main research points are as follows: the reaction mechanism of soot oxidation, development of high-performance catalysts by selecting different carrier types, changing the carrier structure, catalyst loading mode, and doping with different active components. In a study by Uchisawa[11] et al., the performance of Pt catalysts in oxidizing soot under different reaction atmospheres was investigated. The study revealed an important soot oxidation mechanism, in which Pt oxidizes NO to form more oxidizing NO_2, which then facilitates the oxidation of soot. In order to improve the soot catalytic performance of Pt catalysts, the selected catalyst supports are mainly oxides with high specific surface area, good thermal stability, and strong redox performance. The common ones are single Al_2O_3, CeO_2, SiO_2, MnO_x, TiO_2, ZrO_2, or a combination of the above oxides.[12−15] Lee[16] et al. prepared a macroporous Ce oxide support and loaded Ag on the macroporous support to obtain a highly active soot combustion catalyst. Wei[17] et al. prepared a three-dimensional ordered macroporous 3DOM-Al_2O_3-supported Pt catalyst. This support not only improves the degree of contact between soot and active sites but also enhances the catalyst's SO_2 tolerance by providing surface acidity.

Adding a second precious metal or other active components in a Pt catalyst is a common method to improve its soot catalytic performance. The CDPF catalyst with Pd added to the Pt catalyst is widely used in engineering and can inhibit the sintering of Pt particles during the aging process. Studies such as Johns[18] have shown that Pt is easy to sinter at high temperatures. Adding Pt with Pd can help slow down the sintering rate of Pt at higher temperatures. Ho[19] et al. studied Pt/Pd oxidation catalysts for diesel engines and found that bimetallic catalysts can form Pt/Pd alloys so that Pd has more oxidation states. Additionally, bimetallic catalysts exhibit improved resistance to sulfur poisoning. Wei[20] studied the soot oxidation performance of Pt/Pd catalysts supported on TiO_2. Studies have shown that the combination of Pt and Pd exhibits a synergistic ability to activate O_2, resulting in superior catalytic performance and thermal stability. Its T_{10} is only 262 °C. In addition, adding non-precious metal additive elements such as Ce, La, Co, Mn, Cu, K, etc. to Pt catalysts is a research hotspot for scholars.[21−25]

The effects of the active components in Pt/Pd bimetallic catalysts are not simply additive but rather exhibit different synergistic effects depending on the specific ratios used. The synergistic effects of Pt/Pd bimetallic catalysts on catalyzing gaseous pollutants such as CO, HC, etc. have been extensively studied. Several studies have investigated the effect of Pt/Pd ratios on the oxidation of CO and HC.[26−29] For instance,

Zhang[27] et al. discovered that the ignition temperature (T_{50}) of CO and C_3H_6 increased as the Pt/Pd ratio increased. Kang[29] et al. also examined the impact of Pt/Pd ratios on the oxidation of CO and hydrocarbons. When only CO or C_2H_6 was catalyzed, the catalytic activity increased as the Pd content increased. However, when oxidizing mixed gas containing CO, C_2H_4, and C_7H_8, the presence of CO will inhibit the oxidation of C_2H_4 and C_7H_8 by the Pt/Pd catalyst. Additionally, some studies have found that Pd can enhance the heat resistance of bimetallic catalysts, which can slow down the sintering of Pt particles.[30,31]

At present, the performance research of powdered CDPF catalysts is mainly carried out through microscopic characterization tests, temperature-programmed oxidation (TPO), and TG activity tests. In recent years, density functional theory (DFT) calculations have been widely used to study the characteristics of catalyst oxidation soot. Wu[32] et al. calculated the effects of Mn, Fe, Co, Ni, and Cu on the catalytic activity of Pt-TMO for soot combustion by using density functional theory. The reaction mechanism of Nox-assisted soot oxidation has also been determined. Li[33] et al. performed DFT calculations on Pt/Fe_2O_3 catalysts. And it has been found that the active sites on the $Fe_2O_{3\{113\}}$ interface can promote the oxidation of NO to NO_2, making the catalyst highly efficient in soot purification. Lee[34] et al. conducted experiments and used DFT calculations to study the effect of various precious metals (Ag, Au, Pd, Pt, Rh) on the CeO_2-enhanced soot oxidation activity. Lee[35] et al. studied the effect of adding La on the activity of the catalyst to oxidize soot. Through DFT calculations, it was found that excessive La induced the sintering of Ag particles, which led to the reduction of peroxide formation. Wang[36] et al. investigated the oxygen mobility of CeO_2 during soot oxidation through experiments and DFT calculations. Li[37] used this method to study the electron-transfer mechanism during the oxidation of soot. Wang[38] et al. used the DFT method to prove that oxygen vacancies and alkali metals can promote the soot combustion activity of CeO_2. Wang[39] et al. prepared α-MnO_2 catalysts with different morphologies and studied their soot oxidation performance through experiments and DFT methods. DFT calculation results showed that the oxygen vacancies on the catalysts improved the adsorption of reactants, improving the catalytic performance of the catalyst.

As can be seen from the above research status, researchers have carried out a lot of research on the physical and chemical properties of Pt catalysts and soot oxidation characteristics. However, less attention has been paid to the synergistic effect of Pt/Pd, especially the research on the soot combustion characteristics of catalysts with different Pt/Pd ratios has not been reported. In this paper, four kinds of Pt/Pd catalysts were prepared. Through physical and chemical characterization tests, activity test, and DFT calculation, the effect of the Pt/Pd ratio on the catalytic activity for soot combustion was investigated. The Pt/Pd ratio of the catalyst with the best catalytic performance was found. Based on this, the way to reduce the cost of CDPF catalyst was explored. The catalysts were studied by X-ray diffraction (XRD), X-ray photoelectron spectroscopy (XPS), Brunauer−Emmett−Teller (BET) analysis, transmission electron microscopy (TEM), and scanning electron microscopy (SEM). Meanwhile, the soot oxidation activity of catalysts with different Pt/Pd ratios was evaluated by TPO and thermogravimetric (TG) tests. DFT calculations were also performed to correlate the results.

2. EXPERIMENTAL SECTION

2.1. Catalyst Preparation. In this study, four catalyst samples were prepared by loading the precious metals Pt and Pd onto alumina powder in different mass ratios. The total mass fraction of precious metals in the catalysts was kept constant at 1 wt %, regardless of the Pt/Pd mass ratio. Table 1 shows the mass ratios and major components of the precious metals in the four catalysts.

Table 1. Main Component Content of Samples

no	catalyst ratio	Pt mass/g	Pd mass/g	Al_2O_3 mass/g
P1	Pt/Pd = 1:0	0.05	0	5
P2	Pt/Pd = 10:1	0.048	0.0048	5
P3	Pt/Pd = 5:1	0.0435	0.009	5
P4	Pt/Pd = 1:1	0.0262	0.0262	5

The specific preparation process of the catalysts is as follows. $Pt(NH_3)_4(NO_3)_2$ and $Pd(NO_3)_2$ were used as the precursors for Pt and Pd, respectively. The precursors were dissolved and dispersed in deionized water to obtain Pt-based catalyst slurry and Pd-based catalyst slurry, with a precious metal density of 30 g/ft³. When preparing the catalysts using the impregnation method, the loading of precious metals was 100 g/L for both Pt- and Pd-based slurries. According to the requirements of the components listed in Table 1, the corresponding amounts of Pt-based catalyst slurry and Pd-based catalyst slurry were impregnated and dispersed onto γ-Al_2O_3 to ensure that the catalysts were distributed in the pores of the alumina porous material. Subsequently, the samples were dried at 125 °C for 1 h. After drying, the samples were placed in a muffle furnace and calcined at 600 °C for 1.5 h with a heating rate of 30 °C/min and an air atmosphere during the calcination process. The desired catalysts were obtained after calcination.

2.2. Catalyst Characterization. By performing XRD on the sample, information such as the composition and phase structure of the material can be obtained. The analyses were conducted in the scanning range of 10−90° by employing Cu Kα irradiation (λ = 1.5418 Å, k = 0.1528). The catalysts' morphology was analyzed using a Hitachi SU8220 field-emission scanning electron microscope. The XPS technique can obtain the elemental composition and chemical state of the material surface by irradiating the sample with high-energy photons. The distribution of Pt and Pd on Al_2O_3 was confirmed using a Talos F200S transmission electron microscope. The catalyst powder was dispersed in ethanol solution by ultrasonication and deposited onto a thin copper grid before being dried. The specific surface area and pore structure parameters of the powder samples were determined using a physical adsorption instrument, Quantachrome NOVA2000e.The test was carried out by a X-ray photoelectron spectrometer (Thermo Fischer, ESCALAB Xi+, USA). The vacuum degree of the analysis chamber was 8×10^{-10} Pa, and the excitation source was Al Kα ray (hν = 1486.6 eV).

2.3. Activity Test of Catalysts. *2.3.1. TG/DTG Test.* In the TG test, the total amount of soot and catalyst used was 6 mg. The catalyst and soot were stirred evenly, while maintaining a loose contact state between the two. According to the different soot content in the samples, five test schemes were set up for each catalyst sample to investigate the influence of different soot mass ratios on the soot combustion activity. The mass ratios of catalyst and soot in the five schemes are shown in Table 2 as follows.

Table 2. Mass Ratio of Catalyst to Soot in TG Test

program	catalyst/mg	soot/mg
case1	5	1
case2	4	2
case3	3	3
case4	2	4
case5	1	5

The TG/DTG curve was obtained by a TG 209 F1 Libra instrument, which was used to determine the soot combustion performance of the catalyst. The test was carried out in an atmosphere of 13% O_2 and 87% N_2, which simulated the actual oxygen content in the exhaust gas of a diesel engine. The flow rate of working gas was 50 mL/min, and the heating rate was 10 °C/min. The temperature range was 30−850 °C. The activity of the catalyst was evaluated by the characteristic temperature in the TG test: T_i, T_m, T_f. T_i is the temperature at which the mass loss of soot reaches 10% of the total mass of soot, which is the ignition temperature of soot. T_m is the temperature corresponding to the lowest point of the DTG curve. And T_f is the temperature corresponding to the mass loss of soot reaching 90% of the total mass of soot, also known as the burnout temperature of soot.

2.3.2. TPO Test. The TPO test was conducted to analyze the catalytic oxidation activity of the catalyst sample. The total mass of the test sample was 100 mg, with a mass ratio of soot to catalyst of 1:10. The two were loosely mixed. The sample was placed in the middle of a quartz tube. The combustion atmosphere was NO−O_2−N_2 (1000 ppm NO, 10% O_2, and N_2 as the balance gas), and the gas flow rate was set at 500 mL/min. The temperature was controlled by a programmed heating rate of 5 °C/min, with the test sample raised from 50 to 650 °C. An infrared gas analyzer recorded the changes in CO and CO_2 concentrations in the reaction gas in real time.

In this experiment, temperatures T_{10}, T_{50}, and T_{90} were used to evaluate the activity of the catalyst. These temperatures represent the combustion temperatures at which the soot conversion rate in the TPO experiment were 10, 50, and 90%, respectively. The calculation formula of the soot conversion rate[40] is shown in eq 1. In the equation, $[CO_2]_t + [CO]_t$ is the integrated area of the CO_2 and CO curve at a certain temperature. $[CO_2]_T + [CO]_T$ is the integrated total area of the CO_2 and CO curves. Additionally, $S_{CO_2}^p$ represents the selectivity of CO_2 formation when the CO_2 concentration is at its maximum. The selectivity of generating CO_2 is calculated as eq 2

$$X\% = \frac{[CO_2]_t + [CO]_t}{[CO_2]_T + [CO]_T} \qquad (1)$$

$$S_{CO_2}^p = \frac{[CO_2]p}{[CO_2]p + [CO]p} \qquad (2)$$

2.4. DFT Calculation. This study used the first−principle plane wave ultrasoft pseudopotential research method based on density functional theory. The interactions of C and O_2 molecules with Pt_{111} surfaces and Pd-doped Pt_{111} surfaces were studied computationally. The calculations were performed using the CASTEP module[41] in the Materials Studio software package. The generalized gradient approximation (GGA) was used for the exchange−correlation function in the structural optimization of the established periodic plate model. And the

PBE gradient correction function was used for the pseudopotential function.[42] The plane wave cutoff energy was 450 eV. The lattice parameter of the geometrically optimized Pt cell was 0.396 nm, and the experimental value was 0.392 nm.[43] The theoretical calculation results were close to the experimental values, which shows that the calculation accuracy is high. Using a 2 × 2 supercell, one carbon atom was adsorbed on the surface, corresponding to a coverage of 0.25ML. The Brillouin zone k-point grid setting used the Monkhorst−Pack method, and the k-point value was 4 × 4 × 1. The vacuum layer thickness was set to 10 Å to avoid interactions between surfaces. The convergence standard of each atomic force was 0.05 eV/Å. The energy convergence value during geometric optimization calculation was 1×10^{-5} eV/atom. Since the ground state of O_2 is a triplet state, in the part involving the adsorption of O_2 the calculation considers spin polarization. The initial magnetic moment of each oxygen atom was set to 1.

The XRD characterization results presented in this paper reveal that the predominant crystal plane of metal Pt is Pt_{111}. Therefore, calculations were performed using the Pt_{111} plane. First, four periodic layers of Pt_{111} surface were constructed, then the bottom two layers of the surface were fixed, while the top two layers of atoms and the adsorbent were relaxed. To describe the Pd-doped Pt surface, the method used was to replace a certain number of Pt atoms in the first layer of the Pt_{111} surface with Pd atoms. According to the Pt/Pd mass ratios of 1:0, 10:1, 5:1, and 1:1, the 4 Pt atoms in the first layer of the Pt_{111} surface were replaced by Pd. By calculation, the surface was doped with 0, 1, 2, and 3 Pd atoms in sequence.

The calculation of adsorption energy in this paper is based on the following formula

$$E_{ads} = E_{tot} - E_{slab} - E_{C/O_2} \tag{3}$$

E_{ads} is the adsorption energy. E_{tot} is the total energy of the system after adsorbing C atoms or O_2. E_{slab} is the energy of the surface without adsorbed C atoms or O_2. E_{C/O_2} is the energy of a single carbon atom or oxygen molecule. A smaller E_{ads} value indicates a stronger adsorption performance and a more stable structure.

3. RESULTS AND DISCUSSION

3.1. Catalyst Characterization. *3.1.1. XRD Analysis.*
Figure 1 shows the XRD patterns of catalyst samples with four different Pt/Pd ratios. The most abundant phase in the four samples is Al_2O_3, with three different crystal phases observed.
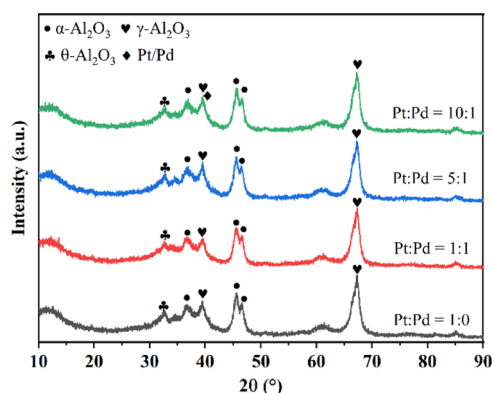

Figure 1. XRD pattern.

All four samples showed strong diffraction peaks of γ-Al_2O_3 at $2\theta = 39.4$ and $67.3°$. It shows the diffraction peak of θ-Al_2O_3 at $2\theta = 32.5°$. The diffraction peaks of α-Al_2O_3 are shown at $2\theta = 45.9$ and $46.6°$. The main crystal phase of Al_2O_3 in the four samples is γ-Al_2O_3, which is an excellent catalyst material with high activity due to its high specific surface area and good stability. The weak characteristic peak at $2\theta \approx 39.79°$ in the figure is between the diffraction peaks of the Pt_{111} and Pd_{111} planes. For samples with Pt/Pd = 1:0, this peak is Pt_{111} surface, while for samples containing Pd, the characteristic peaks can be attributed to the surfaces of both Pt_{111} and Pd_{111}. The weak diffraction peak intensity of Pt and Pd in the sample suggests that the Pt and Pd phases may exist separately, or they may form a Pt−Pd alloy.[44] The weak diffraction peaks of Pt and Pd in the sample also indicate a high dispersion of Pt and Pd on the surface of the carrier.

3.1.2. SEM and BET Analyses. Figure 2 shows SEM images of four kinds of Pt/Pd ratio catalyst powders. The flocculent
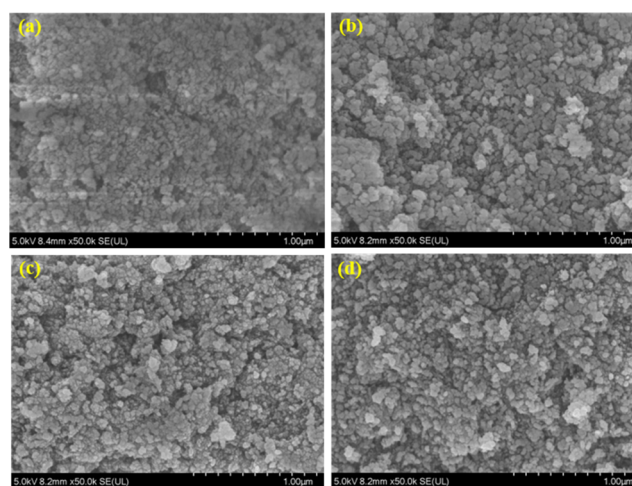

Figure 2. SEM of samples P1 (a), P2 (b), P3 (c), and P4 (d).

particles observed in (a−d) have a loose and porous structure, which suggests that they are made of alumina. However, Pt and Pd particles cannot be observed due to their small size. In Figure 2a, the particle size is approximately 20 nm, and some particles are agglomerated to form blocks. In Figure 2b, there are more lumps than in (a), and most particles are larger than 50 nm. Samples (c,d) have similar shapes, with block and granular alumina evenly distributed. Additionally, particle size in (c,d) is smaller than in (b), but larger than in (a), at around 40 nm. The flocculent and porous structure of alumina in the figure has a large specific surface area, which can enhance the mass-transfer effect and improve catalyst performance.

Figure 3 shows the specific surface area and pore volume data of the four catalyst samples. When both Pt and Pd are present in the catalyst, as the Pd content increases and the Pt content decreases, the specific surface areas and pore volumes of P2, P3, and P4 all gradually decrease. P1, which does not contain Pd, has the smallest specific surface area, while P2 has the largest specific surface area and pore volume among the four samples. Comparing the specific surface area of the four samples, it can be seen that adding Pd to Pt-containing catalysts can increase the specific surface area of the sample. Based on the pore volume data of P1 and P2, it is known that adding a small amount of Pd can increase the pore volume of the catalyst. The pore volume of P3 and P4 is smaller than that
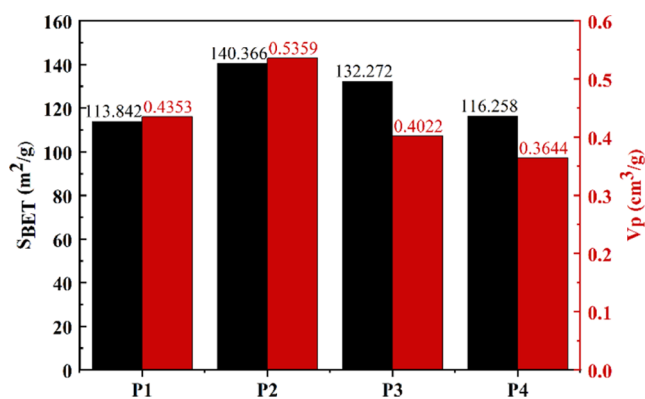
Figure 3. Specific surface areas and pore volumes of samples P1, P2, P3, and P4.

of P1. Therefore, when the Pd content increases to a certain extent, the pore volume of the sample will decrease instead. The reason for the increase in pore volume of P2 after adding Pd relative to P1 may be that some of the Pt and Pd active particles agglomerate together, making it difficult to enter the pores of the catalyst. This reduces the number of dispersed active particles entering the pores, and the pore volume of P2 increases. However, as the Pd content increases, the total number of active particles increases. Compared with the agglomerated active particles, more dispersed Pt and Pd active particles enter the pores of the catalyst, covering the pore

structure, resulting in a decrease in the pore volume of P3 and P4 compared to P1 and P2.[45]

A larger specific surface area is generally considered to provide more active sites for catalytic reactions, which helps catalysts to adsorb reactants and enhance their catalytic activity. According to the data in Figure 3, it can be preliminarily concluded that sample P2 has the best soot catalytic activity among the four samples.

3.1.3. TEM Analysis. As the main difference between the four samples is the variation in the Pt/Pd mass ratio, samples P1 and P4 were selected for characterization analysis. Figure 4a shows that Pt particles are dispersed on the surface of the alumina support. The particles in P1 are small, with a particle size ranging from 0.5 to 2 nm. Figure (b) shows lattice fringes of Pt with a spacing of 0.229 nm, corresponding to the (111) plane of Pt. The EDS mapping images (c,d) of sample P1 demonstrate the uniform dispersion of Pt on the alumina support without any apparent aggregation. In the HRTEM image of sample P4 (e), metallic Pt and Pd particles can be observed. Moreover, Figure (f) demonstrates that noble metals in P4 exhibit more significant aggregation than P1. The spectrum of P4 reveals that the Pt and Pd particles are uniformly dispersed on the alumina support, with a Pt/Pd mass ratio of 1:1. Furthermore, both Pt and Pd coexist in the more aggregated regions, which suggests the formation of independent site structures due to overlap.

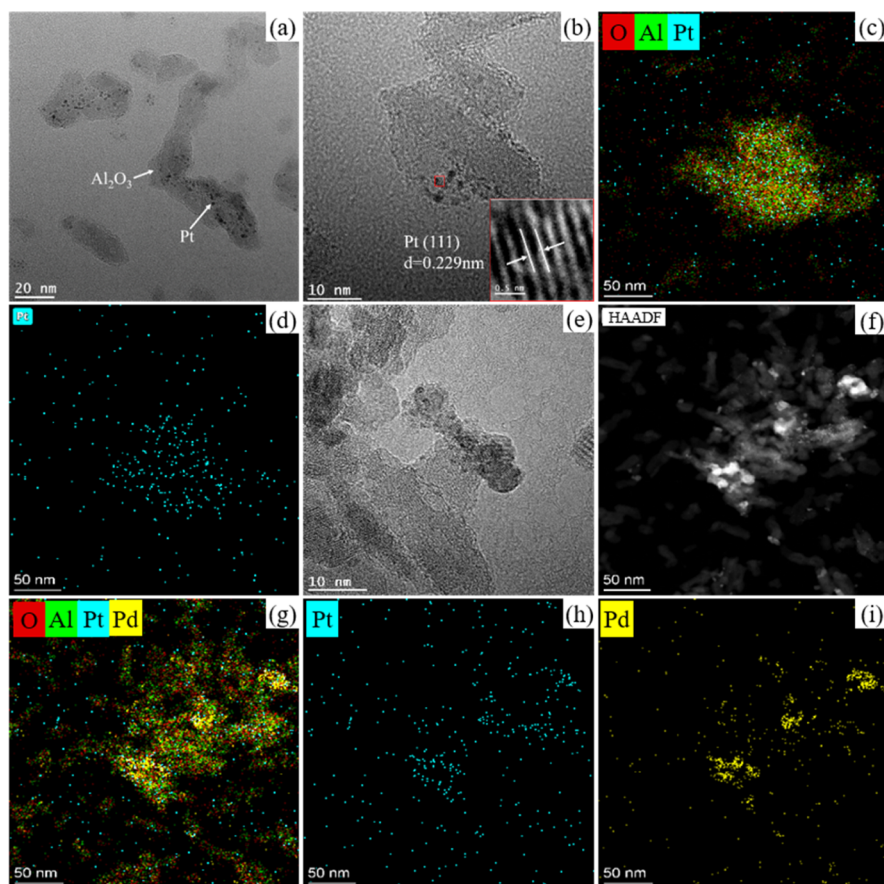*3.1.4. XPS Analysis.* XPS can be used to determine the elemental composition and valence state of the sample surface.

Figure 4. (a) TEM image of P1, (b) HRTEM image of P1. (c,d) EDS mapping of P1. (e) HRTEM image of P4. (f) HAADF image of P4. (g–i) EDS mapping of P4.

Due to the presence of Al and the low Pt content in the sample, as well as the overlapping Al 2p and Pt 4f peaks, the determination result of Pt element is not ideal. In addition, the low Pd content in samples P2 and P3 resulted in the instrument's failure to detect the signal of the Pd element in P2 and P3. Therefore, only the Pd element in sample P4 was analyzed. Figure 5a shows the XPS spectrum of the P4
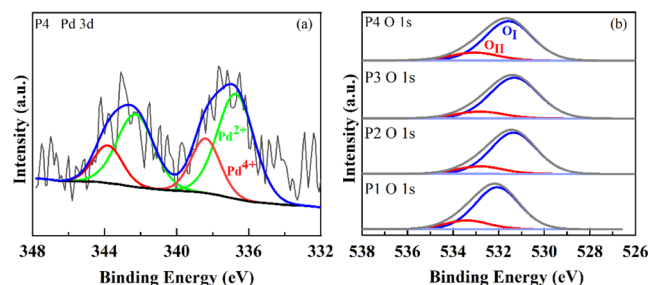

Figure 5. (a) XPS spectra of Pd 3 of P4 and (b) XPS spectra of P1, P2, P3, and P4.

sample's Pd 3d. The spectrum exhibits two peaks. The characteristic peaks at around 338.4 and 343.8 eV correspond to Pd^{4+}, while the peaks at around 336.7 and 342.3 eV correspond to Pd^{2+}. Based on the valence state distribution of the Pd element, Pd species exist in the form of PdO and PdO_2 in the catalyst samples. By integrating the partial spectrum of Pd 3d, the ratio of Pd^{4+}/Pd^{2+} can be calculated. Pd^{4+} in P4 accounts for 29%. It is apparent that the primary form of Pd in sample P4 is PdO. Since the difference between P2, P3, and P4 is only the Pd content, it is not difficult to conclude that Pd in all three samples exists in two valence states of +4 and +2, with the main valence state being +2. Yazawa[46] et al. also got the same conclusion. They pointed out by XPS characterization that the valence state of Pd on the Al_2O_3 coating is mainly +2.

Figure 5b shows the XPS spectra of O 1s in 4 samples. There are two types of oxygen species on the surface of the four catalysts. Oxygen species O_I with binding energy in the range of 532.0−531.3 eV corresponds to lattice oxygen O^{2-}. Additionally, oxygen species O_{II} with binding energy in the range of 533.3−532.8 eV belongs to surface-adsorbed oxygen and weakly adsorbed oxygen O^-. Adsorbed oxygen has high mobility and oxidation reactivity. The content of adsorbed oxygen reflects the oxygen vacancies of the catalyst, which are the active centers of the oxidation reaction.[47] The number of oxygen vacancies can be estimated by the relative concentration ratio O_{II}/O_I. The O_{II}/O_I ratios of P1, P2, P3, and P4 surfaces were 0.19, 0.21, 0.18, and 0.16, respectively. Catalyst P2 has the largest O_{II}/O_I value, indicating the highest number of oxygen vacancies and the greatest density of soot combustion active centers. Therefore, this catalyst can accelerate the generation, migration, and conversion of active oxygen, resulting in better soot catalytic oxidation activity.

3.2. Catalyst Activity Evaluation. *3.2.1. TPO Analysis.* Figure 6 shows the TPO test results for the catalytic combustion of soot using four different catalysts. Figure 6a displays the curve of CO_2 concentration as a function of temperature, while Figure 6b shows the curve of soot conversion rate. The characteristic parameters of catalytic performance, such as T_{10}, T_{50}, and T_{90}, obtained from the TPO experiment are listed in Table 3. As shown in Figure 6a, the CO_2 concentration curves for Pt-based catalysts with a small amount of added Pd (Pt/Pd = 5:1 and Pt/Pd = 10:1) shift
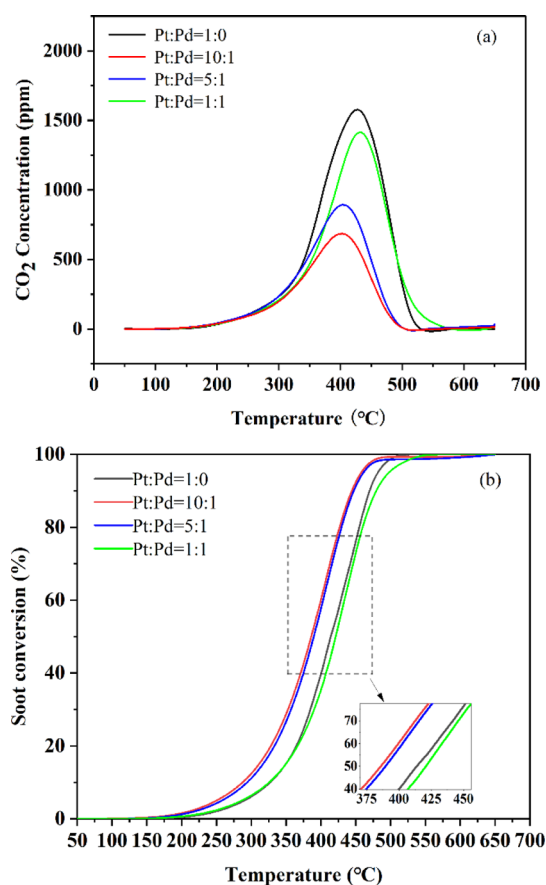

Figure 6. TPO test results of precious metal catalysts with different proportions. (a) CO_2 concentration curve. (b) Soot conversion rate.

Table 3. Catalytic Performance of Samples P1, P2, P3, and P4 on Soot Combustion

sample serial number	P1	P2	P3	P4
catalyst ratio	Pt/Pd = 1:0	Pt/Pd = 10:1	Pt/Pd = 5:1	Pt/Pd = 1:1
T_{10} (°C)	327.03	287.41	294.00	325.45
T_{50} (°C)	413.81	386.04	389.66	420.87
T_{90} (°C)	469.59	444.11	446.90	479.23
$S^P_{CO_2}$ (%)	100	100	100	100

toward lower temperatures. This indicates that adding a small amount of Pd can improve the activity of Pt-based catalysts. According to Table 3, P4 has the highest T_{50} among the four samples, which is 420.87, 7.06 °C higher than the corresponding temperature of P1. In addition, the CO_2 conversion rate curve of P4 in Figure 6b shifts toward the high-temperature region compared to that of P1. All of these results indicate that, compared to catalysts without Pd, the activity of the Pt-based catalyst decreases when the Pt/Pd ratio is 1:1. The addition of a small amount of Pd to the Pt catalyst can significantly improve its activity, but when Pd is added in large amounts, the activity of the catalyst decreases instead. T_{50} is the most critical indicator to measure the soot combustion activity. The T_{50} values for samples P1, P2, P3, and P4 in Table 3 are 413.81, 386.04, 389.66, and 420.87 °C, respectively. The activity order of the four samples is P2 (Pt/Pd = 10:1) > P3 (Pt/Pd = 5:1) > P1 (Pt/Pd = 1:0) > P4 (Pt/Pd = 1:1). This

result is consistent with the BET characterization results. The addition of a small amount of Pd can increase the specific surface area and pore volume of the Pt-based catalyst, so the activity of the catalyst P2 (Pt/Pd = 10:1) is the strongest. Moreover, as shown in Table 3, there is no difference in the selectivity for the production of CO_2 during the combustion of soot among the four catalysts, which is 100%.

3.2.2. TG/DTG Analysis of Catalyst Proportions on Soot Combustion Activity. Pt/Pd ratios on the combustion activity of soot were analyzed by TG test when the mass ratio of catalyst to soot was 5:1. Figure 7 shows the TG and first-order
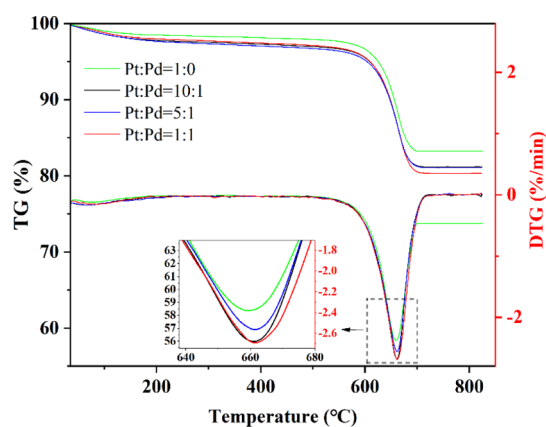

Figure 7. TG-DTG curve of the catalyst.

differential TG (DTG) curves of catalysts with four different Pt/Pd ratios. Table 4 displays the characteristic parameters of

Table 4. Characteristic Parameters of the TG Test of Catalysts

catalyst type	T_i (°C)	T_m (°C)	T_f (°C)
pure soot	607.9	671.5	700.3
Pt/Pd = 1:0	278.5	659.1	678.3
Pt/Pd = 10:1	121.4	661.0	669.6
Pt/Pd = 5:1	122.4	661.4	669.6
Pt/Pd = 1:1	138.8	662.0	669.2

the TG tests of the four catalysts, including T_i, T_m, and T_f. There are two distinct weight loss peaks in Figure 7. When the temperature is ≤ 120 °C, the TG curve shows a gradual descent, while the DTG curve exhibits fluctuations, and the soot loses weight slowly. This stage is attributed to the evaporation of moisture in the soot. At temperatures ranging from 120 to 800 °C, the soot undergoes combustion by oxidation, with the fastest burning rate observed at 600−700 °C. Table 4 shows that the ignition temperature of pure soot is 607.9 °C, the burnout temperature is 700.3 °C, and the temperature corresponding to the maximum DTG change rate is 671.5 °C. After adding Pt and Pd catalysts, the corresponding characteristic temperatures all decreased. Compared with pure carbon soot, the ignition temperature T_i of Pt−Pd catalysts (with ratios of 1:0, 10:1, 5:1, and 1:1) decreased to 329.4, 486.5, 485.5, and 469.1 °C, respectively. The peak combustion temperature T_m decreased by 12.4, 10.5, 10.1, and 9.5 °C, respectively. The burnout temperature T_f decreased by 22, 30.7, 30.7, and 31.1 °C, respectively. Regarding the light-off temperature and burn-out temperature, the addition of Pd can further reduce the light-off temperature

compared with the precious metal Pt, but with an increase of Pd content, the effect of reducing the light-off temperature is weakened. The catalyst with Pt/Pd = 10:1 has the best effect on reducing the light-off temperature. The catalytic performance of catalysts for soot combustion at high temperatures is not outstanding, with only a decrease in characteristic temperature of 10−30 °C. Compared with the pure Pt catalyst, the increase of Pd content makes the peak combustion temperature rise, while the burnout temperature decreases. This indicates that the addition of Pd does not significantly improve the low-temperature activity of Pt-based catalysts but improves the high-temperature activity obviously.

In summary, the optimal catalyst ratio of soot combustion was Pt/Pd = 10:1. This is consistent with the TPO activity test results. The XPS results revealed that catalyst P2 had numerous oxygen vacancies, while the BET test showed that it possessed the largest specific surface area and pore volume. These features were the key reasons for P2's high catalytic activity in soot combustion.

3.2.3. Analysis of Soot Content on the Combustion Activity of Soot. Figure 8 shows the variation of the TGA
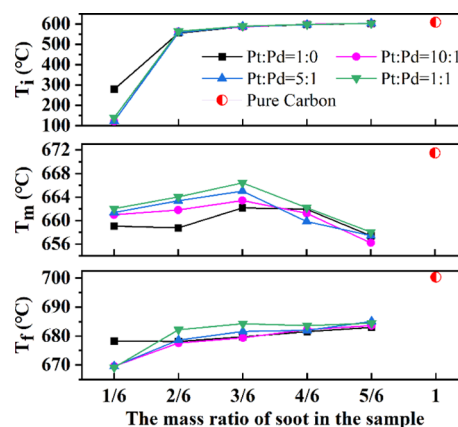

Figure 8. Characteristic temperature of the TG test of catalysts with different proportions under different soot content.

characteristic temperature of each sample with soot content. As the mass ratio of soot in the sample increases, the light-off temperature (T_i) of each catalyst for catalyzing soot combustion gradually increases. When the proportion of soot reaches 5/6, the light-off temperature is about 600 °C, which is close to that of pure soot. At this point, the catalyst's effect on catalyzing the combustion of soot is not significant. Because the amount of soot increases, the contact area between the catalyst and soot decreases. The soot peak combustion temperature (T_m) of catalysts containing Pd increases first and then decreases with the increase of the soot mass ratio. When the mass ratio of soot in the sample reaches 5/6, each catalyst has the best performance in reducing the peak temperature. The catalyst with a Pt/Pd ratio of 10:1 exhibits the most significant effect, lowering the peak temperature by 16 °C compared to pure soot. The lower peak temperature can prevent the diesel particulate filter from overheating during active regeneration. When the mass ratio of soot to the catalyst is 5:1, it can not only enhance the active regeneration performance of DPF loaded with such catalyst but also reduce the usage of precious metals and lower the cost of DPF. As the mass ratio of soot in the sample increases, the burnout temperature of samples containing catalysts gradually increases

Table 5. Surface Structure of Pure Pt$_{111}$ Surface and Pd-Doped Surface

● Pt ● Pd			
Pt$_4$	Pt$_3$Pd$_1$	Pt$_2$Pd$_2$	Pt$_1$Pd$_3$
(a) Pt:Pd=1:0	(b) Pt:Pd=10:1	(c) Pt:Pd=5:1	(d) Pt:Pd=1:1
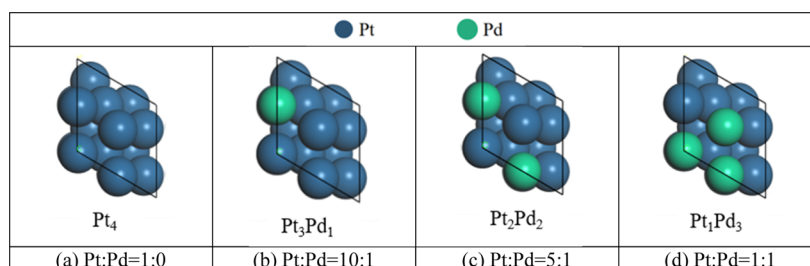
but remains lower than the burnout temperature of pure soot. As the mass fraction of soot increases, the combustion temperature of samples containing the catalyst gradually increases but remains lower than that of pure soot. When the mass fraction of soot is 1/6, the catalyst containing Pd reduces the combustion temperature (T_f) by nearly 10 °C compared to pure Pt catalyst. This highlights the ability of Pd to improve the high-temperature activity of catalysts and makes Pt/Pd catalysts have strong aging resistance. When the mass fraction of soot is increased to 5/6, the combustion temperature of various catalysts for soot combustion increases by 15 °C, but it is still about 15 °C lower than that of pure soot.

3.3. DFT Calculation. Table 5 shows the catalyst surface structure of the pure Pt$_{111}$ and the first layer doped with Pd atoms. In the four figures (a−d), the mass ratio of Pt to Pd in the first layer on the surface is approximately 1:0, 10:1, 5:1, and 1:1, respectively. The x and y in Pt$_x$Pd$_y$ refer to the number of atoms of Pt and Pd in the first layer, respectively. The work function refers to the energy required for an electron to escape from the interior of the system to the surface of the system or the vacuum layer, which can characterize the electron-donating and redox abilities of the catalyst. The work functions (Φ) of surfaces (a−d) are 5.052, 4.942, 4.835, and 4.986 eV, respectively, as shown in Figure 9. Pt$_2$Pd$_2$ has the weakest electron-binding ability, followed by Pt$_3$Pd$_1$, indicating that the surface with Pt/Pd ratios of 5:1 and 10:1 have strong electron-donating abilities.

Adsorption is a prerequisite for catalytic reactions. It is necessary to study the adsorption of reactants on the surface of catalysts. In this study, carbon atoms are utilized to represent soot particles. The adsorption performance of Pt and Pd catalysts with different mass ratios on soot particles is
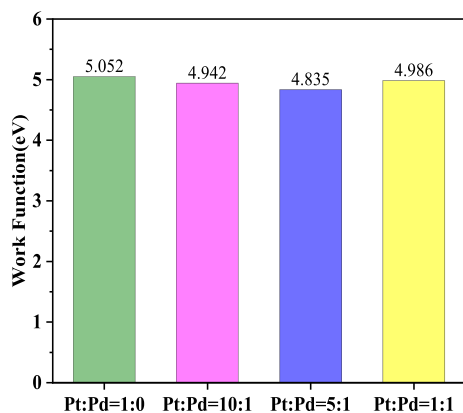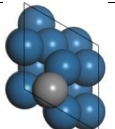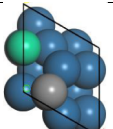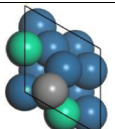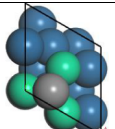
examined through simulation calculations. Table 6 lists the adsorption energy of C atoms on the catalyst surface and the work function of the system. As the number of Pd atoms doped on the surface increases, the value of the adsorption energy first decreases and then increases, indicating that the adsorption performance of the surface on particles increases first and then weakens. The surface doped with one Pd atom has the strongest adsorption performance, followed by the surface doped with two Pd atoms, and the surface doped with three Pd atoms has the weakest adsorption performance. The stronger the adsorption performance, the more conducive it is to the transfer of electrons and acceleration of the activation of reactant molecules. The calculation results suggest that the catalyst surface with a mass ratio of Pt to Pd of 10:1 is more likely to activate carbon atoms and promote the oxidative combustion of soot. The second most effective catalyst surface is with a mass ratio of Pt to Pd of 5:1, and the absolute difference in adsorption energy between the two is only 0.01 eV. This is consistent with the experimental result that the catalyst exhibits the strongest activity in catalyzing the combustion of soot when the mass ratio of Pt to Pd is 10:1 in the TPO test. Furthermore, the surface work function of the Pt$_3$Pd$_1$ catalyst adsorbing C has the largest difference with that of the corresponding clean Pt$_3$Pd$_1$ catalyst, reaching 0.147 eV. When C is adsorbed on the surface of the catalyst, the maximum charge transferred from the interior of the system to the surface occurs, which indicates a stronger bonding between C and Pt.
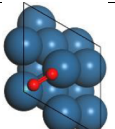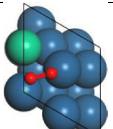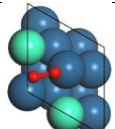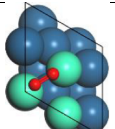
Typically, soot catalytic oxidation mainly follows the Mars-van Krevelen (MvK) mechanism.[48] Therefore, this part also focuses on the adsorption of O$_2$ on each surface, and the results are shown in Table 7. The Pt$_3$Pd$_1$ and Pt$_2$Pd$_2$ surfaces exhibit the strongest adsorption capacity for oxygen, while Pt$_4$ has the weakest. Oxygen in the mass ratio of Pt/Pd of 10:1 and 5:1 is more strongly adsorbed on the catalyst. Taking the difference between the surface work function of the adsorbed oxygen system and the clean surface, it can be seen that Pt$_3$Pd$_1$ and Pt$_2$Pd$_2$ exhibit the greatest differences in work function, reaching 0.765 and 0.792 eV, respectively. Additionally, the simulation calculations reveal that the O−O bond length of oxygen adsorbed on Pt$_3$Pd$_1$ and Pt$_2$Pd$_2$ changes the most, from the initial 1.23 to 1.36 and 1.37 Å, respectively. Therefore, Pt$_3$Pd$_1$ and Pt$_2$Pd$_2$ have more electrons transferring from the interior to the surface when adsorbing oxygen. This phenomenon is favorable for activating the O−O bond (the adsorbed oxygen) and accelerating the production of active oxygen. Based on the simulation results, it is speculated that the catalysts with Pt/Pd mass ratios of 10:1 and 5:1 have more excellent catalytic activity among the four catalysts. This is consistent with the TPO and TG activity test results of the catalysts in this paper.

Figure 9. Surface work function of pure Pt$_{111}$ surface and Pd-doped surface.

Table 6. Adsorption Characteristics of C on Pt$_4$, Pt$_3$Pd$_1$, Pt$_2$Pd$_2$, and Pt$_1$Pd$_3$ Surfaces

structure				
Adsorption energy E(eV)	−8.113	−8.359	−8.349	−7.866
Adsorption system work function Φ(eV)	5.078	4.795	4.758	4.880

adsorption energy E (eV)	−8.113	−8.359	−8.349	−7.866
adsorption system work function Φ (eV)	5.078	4.795	4.758	4.880

Table 7. Adsorption Characteristics of O$_2$ on the Surfaces of Pt$_4$, Pt$_3$Pd$_1$, Pt$_2$Pd$_2$, and Pt$_1$Pd$_3$

structure				
Adsorption energy E(eV)	−0.169	−0.238	−0.297	−0.225
Adsorption system work function Φ(eV)	4.623	4.177	4.043	4.703

adsorption energy E (eV)	−0.169	−0.238	−0.297	−0.225
adsorption system work function Φ (eV)	4.623	4.177	4.043	4.703

4. CONCLUSIONS

This paper investigates the soot catalytic combustion properties of precious metal catalysts with varying Pt−Pd ratios through physicochemical characterization and activity testing. Furthermore, the soot and oxygen adsorption characteristics of the catalysts are examined via DFT. The main findings are as follows. The addition of Pd in small amounts can enhance the catalytic soot combustion activity of the catalyst. However, this effect diminishes as the Pd content increases, and the bimetallic Pt−Pd catalysts can even exhibit weaker soot oxidation activity than pure Pt catalysts. The results of the TPO activity test showed that the order of the activity of catalysts for soot oxidation was Pt/Pd = 10:1 > Pt/Pd = 5:1 > Pt/Pd = 1:0 > Pt/Pd = 1:1. The activity of Pt/Pd = 10:1 is the best, while the activity of Pt/Pd = 1:1 is the worst. The T_{50} of the two are 386.04 and 420.87 °C, respectively. Since the T_{50} difference between the two is 34.84 °C, the catalyst activity difference caused by the different ratios is significant. In addition, the BET test shows that P2 has the largest specific surface area and pore volume. The XPS results show that P2 has the largest number of oxygen vacancies. And the DFT calculation results show that the catalysts with this ratio have strong adsorption of C and O$_2$. The above research results further show that Pt/Pd = 10:1 catalyst has the best soot oxidation activity. The TG test showed that the content of soot had a great influence on the combustion activity of soot. The temperature that best represents the activity of the catalyst is the peak combustion temperature (T_m). With the increase of the soot ratio in the sample, the T_m of each catalyst increases first and then decreases. When the mass ratio of the catalyst to the soot is 5:1, the T_m of the catalysts in each ratio is the lowest, and the activity of the catalysts in oxidizing soot is the best. DFT calculation results show that when the content of Pd doped in the catalyst increases, the adsorption performance of C on the surface of the catalyst model first increases and then

decreases. In addition, oxygen adsorbed more strongly on catalysts with Pt/Pd mass ratios of 10:1 and 5:1. This is confirmed by the results of the activity strength in the TPO activity test.

■ AUTHOR INFORMATION

Corresponding Author

    Yunhua Zhang − *School of Automotive Studies, Tongji University, Shanghai 200092, China;* ⊙ orcid.org/0000-0003-1968-9365; Phone: 0086-18818203238; Email: zhangyunhua131@tongji.edu.cn

Authors

    Diming Lou − *School of Automotive Studies, Tongji University, Shanghai 200092, China*

    Beihong Xiang − *School of Automotive Studies, Tongji University, Shanghai 200092, China*

    Liang Fang − *School of Automotive Studies, Tongji University, Shanghai 200092, China*

    Piqiang Tan − *School of Automotive Studies, Tongji University, Shanghai 200092, China*

    Zhiyuan Hu − *School of Automotive Studies, Tongji University, Shanghai 200092, China;* ⊙ orcid.org/0000-0002-0906-0128

Complete contact information is available at:
https://pubs.acs.org/10.1021/acsomega.3c01543

Notes

The authors declare no competing financial interest.

Technological Innovation Guidance Program (20212BDH80015).

■ REFERENCES

(1) Guan, B.; Zhan, R.; Lin, H.; Huang, Z. Review of the state-of-the-art of exhaust particulate filter technology in internal combustion engines. *J. Environ. Manag.* **2015**, *154*, 225−258.

(2) Chen, C.; Yao, A.; Yao, C.; Qu, G. Experimental study of the active and passive regeneration procedures of a diesel particulate filter in a diesel methanol dual fuel engine. *Fuel* **2020**, *264*, 116801.

(3) Fang, J.; Meng, Z.; Li, J.; Du, Y.; Qin, Y.; Jiang, Y.; Bai, W.; Chase, G. G. The effect of operating parameters on regeneration characteristics and particulate emission characteristics of diesel particulate filters. *Appl. Therm. Eng.* **2019**, *148*, 860−867.

(4) Qi, B.; Li, Z.; Lou, D.; Zhang, Y. Experimental investigation on the effects of DPF Cs-V-based non-precious metal catalysts and their coating forms on non-road diesel engine emission characteristics. *Environ. Sci. Pollut. Res.* **2022**, *30*, 9401−9415.

(5) Yao, P.; Huang, Y.; Jiao, Y.; Xu, H.; Wang, J.; Chen, Y. Soot oxidation over Pt-loaded CeO2-ZrO2 catalysts under gasoline exhaust conditions: Soot-catalyst contact efficiency and Pt chemical state. *Fuel* **2023**, *334*, 126782.

(6) Chen, Z.; Luo, D.; Zhang, H.; Zhang, N.; Li, J.; Gao, B.; Qiu, R.; Li, Y.; Yang, Z. Reaction pathway of nitric oxide oxidation on nanosized Pt/SiO2 catalysts for diesel exhaust purification. *Mol. Catal.* **2021**, *516*, 111991.

(7) Tan, W.; Xie, S.; Wang, X.; Wang, C.; Li, Y.; Shaw, T. E.; Ma, L.; Ehrlich, S. N.; Liu, A.; Ji, J.; et al. Highly efficient Pt catalyst on newly designed CeO2-ZrO2-Al2O3 support for catalytic removal of pollutants from vehicle exhaust. *Chem. Eng. J.* **2021**, *426*, 131855.

(8) Zhao, B.; Chen, W.; Tan, Y.; Li, F.; Tian, M. Preparation of M/Ce1−Ti O2 (M=Pt, Rh, Ru) from sol-gel method and their catalytic oxidation activity for diesel soot. *J. Rare Earths* **2022**, *40*, 1849−1859.

(9) Zhang, S.; Feng, X.; Rao, C.; Xu, X.; Xu, J.; Fang, X.; Li, Y.; Wang, X. Engineering low Pd content catalysts for soot combustion through tuning the Pd-SnO2 interface interaction: Disclosing the critical role of dual Pd valence states for the activity. *Appl. Catal., A* **2022**, *647*, 118906.

(10) Lee, J. H.; Kim, M. J.; Lee, E. J.; Lee, D. W.; Kim, C. H.; Lee, K. Y. Promoting effect of Rh-impregnation on Ag/CeO2 catalyst for soot oxidation. *Appl. Surf. Sci.* **2022**, *572*, 151504.

(11) Oi Uchisawa, J.; Obuchi, A.; Zhao, Z.; Kushiyama, S. Carbon oxidation with platinum supported catalysts. *Appl. Catal., B* **1998**, *18*, L183−L187.

(12) Xiong, J.; Li, Z.; Zhang, P.; Yu, Q.; Li, K.; Zhang, Y.; Zhao, Z.; Liu, J.; Li, J.; Wei, Y. Optimized Pt-MnOx interface in Pt-MnOx/3DOM-Al2O3 catalysts for enhancing catalytic soot combustion. *Chin. Chem. Lett.* **2021**, *32*, 1447−1450.

(13) Li, S.; He, J.; Dan, Y.; Li, X.; Jiao, Y.; Deng, J.; Wang, J.; Chen, Y.; Jiang, L. Bifunctional roles of Nd2O3 on improving the redox property of CeO2−ZrO2−Al2O3 materials. *Mater. Chem. Phys.* **2020**, *240*, 122150.

(14) Wang, H.; Chen, Z.; Chen, D.; Yu, Q.; Yang, W.; Zhou, J.; Wu, S. Facile, template-free synthesis of macroporous SiO2 as catalyst support towards highly enhanced catalytic performance for soot combustion. *Chem. Eng. J.* **2019**, *375*, 121958.

(15) Zhang, P.; Xiong, J.; Wei, Y.; Li, Y.; Zhang, Y.; Tang, J.; Song, W.; Zhao, Z.; Liu, J. Exposed {0 0 1} facet of anatase TiO2 nanocrystals in Ag/TiO2 catalysts for boosting catalytic soot combustion: The facet-dependent activity. *J. Catal.* **2021**, *398*, 109−122.

(16) Lee, J. H.; Lee, S. H.; Choung, J. W.; Kim, C. H.; Lee, K. Y. Ag-incorporated macroporous CeO2 catalysts for soot oxidation: effects of Ag amount on the generation of active oxygen species. *Appl. Catal., B* **2019**, *246*, 356−366.

(17) Wei, Y.; Zhang, P.; Xiong, J.; Yu, Q.; Wu, Q.; Zhao, Z.; Liu, J. SO2-Tolerant Catalytic Removal of Soot Particles over 3D Ordered Macroporous Al2O3-Supported Binary Pt−Co Oxide Catalysts. *Environ. Sci. Technol.* **2020**, *54*, 6947−6956.

(18) Johns, T. R.; Goeke, R. S.; Ashbacher, V.; Thüne, P. C.; Niemantsverdriet, J. W.; Kiefer, B.; Kim, C. H.; Balogh, M. P.; Datye, A. K. Relating adatom emission to improved durability of Pt−Pd diesel oxidation catalysts. *J. Catal.* **2015**, *328*, 151−164.

(19) Ho, P. H.; Shao, J.; Yao, D.; Ilmasani, R. F.; Salam, M. A.; Creaser, D.; Olsson, L. The effect of Pt/Pd ratio on the oxidation activity and resistance to sulfur poisoning for Pt-Pd/BEA diesel oxidation catalysts with high siliceous content. *J. Environ. Chem. Eng.* **2022**, *10*, 108217.

(20) Wei, Y.; Wu, Q.; Xiong, J.; Li, J.; Liu, J.; Zhao, Z.; Hao, S. Efficient catalysts of supported PtPd nanoparticles on 3D ordered macroporous TiO2 for soot combustion: Synergic effect of Pt-Pd binary components. *Catal. Today* **2019**, *327*, 143−153.

(21) Jiao, Y.; He, J.; Li, S.; Yao, P.; Fan, J.; Wang, J.; Chen, Y. The promoting effect of Pt loaded with different redox supports on NONO2 cycle-assisted soot combustion. *Combust. Flame* **2023**, *248*, 112552.

(22) Yi, C.; Fang, J.; Pu, P.; Yang, Y.; Chen, Z.; Zuo, Z.; Han, Z. Insight into catalytic activity of K-Ce catalysts and K-Ce based mixed catalysts on diesel soot combustion. *Mol. Catal.* **2023**, *535*, 112905.

(23) Zeng, L.; Cui, L.; Wang, C.; Guo, W.; Gong, C. In-situ modified the surface of Pt-doped perovskite catalyst for soot oxidation. *J. Hazard Mater.* **2020**, *383*, 121210.

(24) Shao, J.; Lan, X.; Zhang, C.; Cao, C.; Yu, Y. Recent advances in soot combustion catalysts with designed micro-structures. *Chin. Chem. Lett.* **2022**, *33*, 1763−1771.

(25) Camposeco, R.; Zanella, R. Multifunctional Pt-Cu/TiO2 nanostructures and their performance in oxidation of soot, form-aldehyde, and carbon monoxide reactions. *Catal. Today* **2022**, *392*-*393*, 23−30.

(26) Chen, K.; Wan, J.; Wang, T.; Sun, Q.; Zhou, R. Construction of bimetallic Pt−Pd/CeO2−ZrO2−La2O3 catalysts with different Pt/Pd ratios and its structure−activity correlations for three-way catalytic performance. *J. Rare Earths* **2023**, *41*, 896−904.

(27) Zhang, J.; Lou, D.; Sun, Y.; Tan, P.; Hu, Z.; Huang, C. Effects of DOC and CDPF catalyst composition on emission characteristics of light-duty diesel engine with DOC+ CDPF+ SCR system, 2018.

(28) Dong, F.; Yamazaki, K. The Pt-Pd alloy catalyst and enhanced catalytic activity for diesel oxidation. *Catal. Today* **2021**, *376*, 47−54.

(29) Kang, S. B.; Hazlett, M.; Balakotaiah, V.; Kalamaras, C.; Epling, W. Effect of Pt: Pd ratio on CO and hydrocarbon oxidation. *Appl. Catal., B* **2018**, *223*, 67−75.

(30) Morlang, A.; Neuhausen, U.; Klementiev, K. V.; Schütze, F. W.; Miehe, G.; Fuess, H.; Lox, E. S. Bimetallic Pt/Pd diesel oxidation catalysts: Structural characterisation and catalytic behaviour. *Appl. Catal., B* **2005**, *60*, 191−199.

(31) Kaneeda, M.; Iizuka, H.; Hiratsuka, T.; Shinotsuka, N.; Arai, M. Improvement of thermal stability of NO oxidation Pt/Al2O3 catalyst by addition of Pd. *Appl. Catal., B* **2009**, *90*, 564−569.

(32) Wu, Q.; Jing, M.; Wei, Y.; Zhao, Z.; Zhang, X.; Xiong, J.; Liu, J.; Song, W.; Li, J. High-efficient catalysts of core-shell structured Pt@transition metal oxides (TMOs) supported on 3DOM-Al2O3 for soot oxidation: The effect of strong Pt-TMO interaction. *Appl. Catal., B* **2019**, *244*, 628−640.

(33) Li, Y.; Zhang, P.; Xiong, J.; Wei, Y.; Chi, H.; Zhang, Y.; Lai, K.; Zhao, Z.; Deng, J. Facilitating catalytic purification of auto-exhaust carbon particles via the Fe2O3 {113} facet-dependent effect in Pt/Fe2O3 catalysts. *Environ. Sci. Technol.* **2021**, *55*, 16153−16162.

(34) Lee, J. H.; Jo, D. Y.; Choung, J. W.; Kim, C. H.; Ham, H. C.; Lee, K. Y. Roles of noble metals (M= Ag, Au, Pd, Pt and Rh) on CeO2 in enhancing activity toward soot oxidation: Active oxygen species and DFT calculations. *J. Hazard Mater.* **2021**, *403*, 124085.

(35) Lee, J.; Lee, M. W.; Kim, M. J.; Lee, J. H.; Lee, E. J.; Jung, C.; Choung, J. W.; Kim, C. H.; Lee, K. Y. Effects of La incorporation in catalytic activity of Ag/La-CeO2 catalysts for soot oxidation. *J. Hazard Mater.* **2021**, *414*, 125523.

(36) Wang, Y.; Xie, Y.; Zhang, C.; Chen, W.; Wang, J.; Zhang, R.; Yang, H. Tuning the oxygen mobility of CeO2 via Bi-doping for diesel

soot oxidation: Experimental and DFT studies. *J. Environ. Chem. Eng.* **2021**, *9*, 105049.

(37) Li, Q.; Xin, Y.; Zhang, Z.; Cao, X. Electron donation mechanism of superior Cs-supported oxides for catalytic soot combustion. *Chem. Eng. J.* **2018**, *337*, 654−660.

(38) Wang, C.; Yuan, H.; Lu, G.; Wang, H. Oxygen vacancies and alkaline metal boost CeO2 catalyst for enhanced soot combustion activity: A first-principles evidence. *Appl. Catal., B* **2021**, *281*, 119468.

(39) Wang, Y.; Zhang, L.; Zhang, C.; Xu, X.; Xie, Y.; Chen, W.; Wang, J.; Zhang, R. Promoting the Generation of Active Oxygen over Ag-Modified Nanoflower-like α-MnO$_2$ for Soot Oxidation: Experimental and DFT Studies. *Ind. Eng. Chem. Res.* **2020**, *59*, 10407−10417.

(40) Xie, Y.; Zhang, C.; Wang, D.; Lu, J.; Wang, Y.; Wang, J.; Zhang, L.; Zhang, R. Catalytic performance of a Bi2O3−Fe2O3 system in soot combustion. *New J. Chem.* **2019**, *43*, 15368−15374.

(41) Dange, P.; Savla, N.; Pandit, S.; Bobba, R.; Jung, S. P.; Kumar Gupta, P.; Sahni, M.; Prasad, R. A comprehensive review on oxygen reduction reaction in microbial fuel cells. *J. Renewable Mater.* **2022**, *10*, 665−697.

(42) Mombrú, D.; Faccio, R.; Mombrú, Á. W. Possible doping of single-layer MoS2 with Pt: A DFT study. *Appl. Surf. Sci.* **2018**, *462*, 409−416.

(43) Wong, Y.; Choi, Y. H.; Tanaka, S.; Yoshioka, H.; Mukai, K.; Halim, H. H.; Mohamed, A. R.; Inagaki, K.; Hamamoto, Y.; Hamada, I.; et al. Adsorption of CO2 on Terrace, Step, and Defect Sites on Pt Surfaces: A Combined TPD, XPS, and DFT Study. *J. Phys. Chem. C* **2021**, *125*, 23657−23668.

(44) Kim, J.; Kim, Y.; Wiebenga, M. H.; Oh, S. H.; Kim, D. H. Oxidation of C3H8, iso-C5H12 and C3H6 under near-stoichiometric and fuel-lean conditions over aged Pt−Pd/Al2O3 catalysts with different Pt: Pd ratios. *Appl. Catal., B* **2019**, *251*, 283−294.

(45) Guo, Y.; Zhang, S.; Mu, W.; Li, X.; Li, Z. Methanol total oxidation as model reaction for the effects of different Pd content on Pd-Pt/CeO2-Al2O3-TiO2 catalysts. *Mol. Catal.* **2017**, *429*, 18−26.

(46) Yazawa, Y.; Yoshida, H.; Takagi, N.; Komai, S. I.; Satsuma, A.; Hattori, T. Oxidation state of palladium as a factor controlling catalytic activity of Pd/SiO2−Al2O3 in propane combustion. *Appl. Catal., B* **1998**, *19*, 261−266.

(47) Zhao, Z.; Yang, X.; Wu, Y. Comparative study of Nickel-based perovskite-like mixed oxide catalysts for direct decomposition of NO. *Appl. Catal., B* **1996**, *8*, 281−297.

(48) Mori, K.; Jida, H.; Kuwahara, Y.; Yamashita, H. CoOx-decorated CeO2 heterostructures: effects of morphology on their catalytic properties in diesel soot combustion. *Nanoscale* **2020**, *12*, 1779−1789.